Received: 31 March 2022 | Revised: 22 September 2022 | Accepted: 27 September 2022

DOI: 10.1002/hyp.14726

IN HONOUR OF DES WALLING

WILEY

Using particle size distributions to fingerprint suspended sediment sources—Evaluation at laboratory and catchment scales

Niels F. Lake[1,2] | Núria Martínez-Carreras[1] | Peter J. Shaw[2] | Adrian L. Collins[3]

[1]Catchment and Eco-hydrology Research Group (CAT), Environmental Research and Innovation (ERIN) department, Luxembourg Institute of Science and Technology (LIST), Belvaux, Luxembourg

[2]Centre for Environmental Science, School of Geography and Environmental Science, University of Southampton, Southampton, UK

[3]Net Zero and Resilient Farming, Rothamsted Research, North Wyke, UK

Correspondence
Niels F. Lake, Catchment and Eco-hydrology Research Group (CAT), Environmental Research and Innovation (ERIN) department, Luxembourg Institute of Science and Technology (LIST), 41 rue du Brill, L-4422 Belvaux, Luxembourg.
Email: niels.lake@list.lu

Funding information
Luxembourg National Research Fund (FNR), Grant/Award Number: C17/SR/11699372

Abstract

Applications of sediment source fingerprinting studies are growing globally despite the high costs and workloads associated with the analyses of conventional fingerprint properties on target sediment samples collected using traditional methods. To this end, there is a need to test new fingerprint properties that can overcome these challenges. Sediment particle size could potentially contribute here since it is relatively easy to measure but, until now, has rarely been deployed as a fingerprint itself. Instead, particle size has been used to ensure that source and target sediment samples are more directly comparable on the basis of the fingerprints used. Accordingly, this work examined whether particle size distributions (PSDs) could be used as a reliable fingerprint for apportioning sediment sources, in combination with a grain size un-mixing model. Application of PSDs as a fingerprint was tested at two scales: (i) in a laboratory setting where soil samples with known PSDs were used to generate artificial mixtures to evaluate un-mixing model results, and (ii) a catchment setting comparing PSDs in a confluence-based approach to test if downstream target sediment PSDs could be un-mixed into the contributions of sediment coming from an upstream and a tributary sampling site. Laboratory results showed that the known proportions of the two, three and four soil samples in the artificial mixtures were predicted accurately using the AnalySize grain size un-mixing model, giving average absolute errors of 9%, 8% and 6%, respectively. Catchment results showed variable performances when comparing un-mixing results with sediment budget estimations, with the best results obtained at higher discharge values during storm runoff events. Overall, our results suggest the potential of using PSDs for estimating contributions of sediment sources delivering SS with distinct PSDs when sources are located at short distance to the downstream sampling site.

KEYWORDS
AnalySize, end-member mixing model, grain size distribution, sediment fingerprinting, sediment origin

1 | INTRODUCTION

Information on sediment origin can help target remedial actions to mitigate erosion in river catchments (Belmont et al., 2011). The sediment fingerprinting approach is a widely-adopted method to assemble this information, allowing the quantification of the relative contributions of different sources to target suspended sediment (SS) collected downstream (see reviews by e.g., Collins et al., 2020, 2017; Haddadchi et al., 2013; Owens et al., 2016). To apply the method, both source and SS samples need to be collected. Potential sources are normally sampled manually, while SS is often collected using time-integrated sediment traps (e.g., García-Comendador et al., 2021; Pulley & Collins, 2021), or automatic water samplers (e.g., Legout et al., 2021; Vale et al., 2020). Selected properties or 'fingerprints' are then measured on the SS and compared with the corresponding fingerprint values measured on the potential source samples. This comparison allows for estimations of the relative contribution of each source to the target SS using un-mixing models.

A wide range of soil and sediment properties has been used for source fingerprinting, for example, geochemistry, fallout radionuclides, colour properties, stable isotopes, compound specific stable isotopes, and mineral magnetic properties (e.g., Blake et al., 2012; Collins et al., 1997a; Martínez-Carreras et al., 2010; Oldfield et al., 1985; Revel-Rolland et al., 2005; Upadhayay et al., 2022; Wallbrink et al., 1998). A common issue is selecting the particle size fraction to analyse (e.g., Collins et al., 2017; Koiter et al., 2018, 2013; Laceby et al., 2017; Smith & Blake, 2014). This relates to the essence of an effective fingerprinting property, where fingerprints must both differentiate between sources while behaving conservatively (Walling et al., 1993). However, fingerprint values often vary with particle size in a non-linear manner that is difficult to generalize (Horowitz & Elrick, 1987; Russell et al., 2001). For instance, total organic carbon (Wynn et al., 2005) and radionuclides (Horowitz & Elrick, 1987) are generally enriched in the finer particle size fractions, while different mineral magnetic properties (e.g., Hatfield & Maher, 2009) and colour parameters (e.g., Pulley & Rowntree, 2016) are linked to different particle size fractions.

Various approaches have been adopted to account for particle size in sediment fingerprinting studies to facilitate direct comparison between the properties of target SS and possible sources. The most commonly-applied approach is to fractionate SS and source samples by sieving (Laceby et al., 2017). Here, source materials and target SS samples are commonly sieved to <63 μm (Walling et al., 1993), since this fraction is considered to account for most of the SS load transported by rivers (e.g., Legout et al., 2013; Walling et al., 2000). In other studies, samples are sieved to different fractions and separate fingerprint analyses performed for isolated fractions (e.g., Gaspar et al., 2022, 2019; Motha et al., 2002). Another approach is to sieve and then apply correction factors (e.g., Collins et al., 1997b; He & Walling, 1996). However, the underlying assumptions used for these correction factors were challenged by Smith and Blake (2014) due to the fact that positive linear relationships between particle size and fingerprint concentrations do not apply to all fingerprint properties (Horowitz, 1991; Russell et al., 2001). Given these uncertainties, recent reviews have stressed the need to consider both the most representative particle size fraction for the target sediment in question and to examine dependency of fingerprint properties on particle size, especially where a broad size fraction is used (Collins et al., 2017).

Alternatively, the confluence-based sediment fingerprinting approach has been proposed to facilitate direct comparison between the properties of downstream target SS samples and possible sources (i.e., different tributaries used to represent upstream catchment sources) (Collins et al., 1996; Collins et al., 1997c; Nosrati et al., 2018; Nosrati et al., 2019; Patault et al., 2019; Vale et al., 2016). Here, uncertainties regarding which particle size fractions are delivered from hillslope sources to streams are minimized, reducing potential uncertainties associated with particle size enrichment or depletion and the concomitant effects on fingerprint properties (Laceby et al., 2017). However, in-stream hydrodynamic processes result in mobilization of different SS size fractions and affect SS flocculation, that might still cause uncertainty as to which particle sizes are present at different sections of the stream (e.g., Droppo, 2004; Grangeon et al., 2014), challenging fingerprint conservation.

While the consideration of particle size in sediment fingerprinting is mainly limited to investigating its controls on fingerprint values, there is evidence that particle size can be used directly as a fingerprint property or tracer (Kranck & Milligan, 1985; Laceby et al., 2017). For example, Vale et al. (2016) applied a confluence-based approach to the Manawatu River catchment (New Zealand), collecting fine sediments from the riverbed using a trowel. The authors showed that varying rock types, situated in different sub-catchments and drained by different tributaries, were linked to differences in SS D_{50} values. In the same catchment, Vale et al. (2020) linked patterns in SS dynamics during storm events to differences in particle sizes. They argued that the finer particle size of mudstone (D_{50} of 16 μm) likely allowed prolonged entrainment in the water during storm events, whereas the transport of coarser mountain range and unconsolidated sediment (D_{50} of 44 μm) ceased as the storm events progressed. The results of such studies therefore suggest that temporal changes in sediment source contributions can be fingerprinted using observed changes in particle sizes or particle size distributions. Existing work that included particle size for the sole purpose of tracing (Li et al., 2020), reported the use of particle size statistics (e.g., D_{60}, D_{70} and well as clay and silt percentages) for fingerprints to identify sediment sources of core sediment. Another study (Tang et al., 2018) looked at the spatial and temporal variability of SS source particle size input and the effects of sediment size sorting in reservoir dam deposits. Droppo et al. (2005) suggested rather than using particle size, particle shape and fractal dimension could be used to trace SS sources. Furthermore, the idea of using particle size distributions (PSDs) for sediment source fingerprinting purposes was raised in an abstract by Liu et al. (2014), where the possibility to measure PSDs from potential soil sources and compare those with the target SS collected by sediment traps was proposed. A corresponding publication on this proposal has not been found at the time of publication of the present study.

Many recent sediment fingerprinting studies underscore increasing opportunities to measure sediment PSDs. This can be achieved using laboratory equipment such as the Beckman Coulter LS 13320 (Beckman Coulter, Inc., Fullerton, CA) and Mastersizer 3000 (Malvern Instruments Ltd, Worcestershire, UK) laser diffraction particle size analysers (as used by e.g., Patault et al., 2019 and García-Comendador et al., 2021), and in-field equipment such as the LISST sensor (Sequoia Scientific, Bellevue, WA, USA), also based on laser diffraction (as used by e.g., Czuba et al., 2015; Upadhayay et al., 2021). Differences in sediment PSDs are regularly used in sedimentology to infer past sediment provenance and to reconstruct past changes in, for example, climatic conditions or tectonic processes (Beuscher et al., 2017; Dietze et al., 2012). To this end, Weltje (1997) first used PSD data together with an end-member mixing model (EMMA) to estimate the proportions of different sediment sources. Subsequent research led to the development of other end-member grain size un-mixing models such as DRS-unmixer (Heslop et al., 2007), EMMAgeo (Dietze et al., 2012), AnalySize (Paterson & Heslop, 2015), BEMMA (Yu et al., 2016) and BasEMMA (Zhang et al., 2020). These grain-size un-mixing models use the whole PSD data as input, whereas within the sediment fingerprinting community linear multivariate un-mixing models are used most widely (e.g., MixSIAR: Stock et al., 2018; Stock & Semmens, 2016, FingerPro: Lizaga et al., 2020).

We propose the use of tracing contemporary SS sources with PSDs as a fingerprint in combination with an end-member grain size un-mixing model (AnalySize). To this end, we: (i) evaluate un-mixing model performances using artificial laboratory mixtures, with known proportions of soil samples sieved to different size fractions, and; (ii) un-mix target SS samples from a catchment scale confluence-based approach based on differences in upstream source SS PSDs, while relating the un-mixing model performances to differences in upstream source D_{50} values and observed water discharges.

2 | MATERIALS AND METHODS

This study describes two approaches using complementary methods to measure PSD. First, a LISST sensor (Sequoia Scientific, Bellevue, WA, USA) was used in controlled laboratory experiments, where PSDs were measured inside a tank set-up to evaluate the un-mixing model (section 2.1). Second, a Mastersizer instrument (Malvern Instruments Ltd, Worcestershire, UK) was used to measure PSDs in discrete samples collected in a catchment scale field experiment, with the un-mixing model then applied to estimate confluence sediment source contributions (section 2.2). The two approaches were deployed in parallel, not compared directly, with the approaches used according to their different objectives comprising: (1) laboratory experiments aiming to measure in-tank PSDs in specified mixtures of source soils (section 2.1), and; (2) field experiments aiming to measure PSDs after applying ultrasound by taking sub-samples from a well-mixed environment (section 2.2).

2.1 | Laboratory experiments

Laboratory experiments were performed to evaluate the grain-size un-mixing model AnalySize under controlled conditions. Both soil samples and artificial mixtures, composed of these different soil samples, were suspended inside a tank set-up and PSD was measured using a LISST sensor. The PSDs of both the soil samples and mixtures were then used to evaluate the grain-size un-mixing model, according to the known soil sample contributions present in the mixtures. The tank set-up, as well as the soil samples and mixtures, were used previously in Lake et al. (2022) to investigate the feasibility of using absorbance measurements obtained with a submerged spectrophotometer for un-mixing source soil sample contributions.

2.1.1 | Soil samples and artificial mixtures

Soil sampling was carried out at six different sites in Luxembourg (see Table A.1 for details on sampling site coordinates). Sites were selected based on differences in geochemistry and mineralogy (Lake et al., 2022). Soil samples were collected using a trowel, after removal of the top layer of soil (0–5 cm). Care was taken to collect only material that appeared homogeneous in colour. The samples were then dried at room temperature, disaggregated with a pestle and mortar, and sieved into three different size fractions: <32, 32–63 and 63–125 μm. This resulted in 17 soil samples (the 63–125 μm fractions for soil 6 was omitted due to the low quantities present). Soil samples are hereafter indicated by #soil. fraction, with 'soil' representing the soils ($n = 6$), and 'fraction' the sieved particle size fraction (0.1 for <32 μm; 0.2 for 32–63 μm; 0.3 for 63–125 μm). Soil samples were used to create 25 artificial mixtures. The mixtures consisted of two, three or four soil samples, with contributions chosen in order to have a majority of mixtures with a dominant soil sample (Table 1). Mixtures 1–9 were composed of soil samples sieved to different size fractions. Mixtures 10–25 were composed of soil samples sieved to the same particle size fraction. These two approaches were tested to see if both distinct differences in source PSDs (soil sources sieved to different fractions) and small differences in source PSDs (soil sources sieved to same size fraction) could be used for un-mixing.

2.1.2 | Laboratory set-up

A LISST 200X sensor (Sequoia Scientific, Bellevue, WA, United States) was used in the laboratory set-up (Figure 1) to measure PSDs. This sensor uses laser diffraction technology, whereby particles of different sizes diffract the laser beam at different angles (Agrawal & Pottsmith, 2000). The diffracted light is assigned to one of the 36 particle size classes, providing PSDs on the soil samples and mixtures tested (in the 1–500 μm range). The output value in each size class is given in $\mu L\ L^{-1}$. Output values were converted into percentage of volume concentration to allow comparison between different

TABLE 1 Soil sample input contributions (%) for the mixtures 1–9, based on theoretical input contributions, and adapted input contributions (bold), based on measured concentrations in the tank set-up

	Mixture No.	Soil sample (%)	Soil sample (%)	Soil sample (%)	Soil sample (%)
Mixtures of samples sieved to different size fractions:					
Two soil samples	1	#3.1 (80) **(81.6)**	#4.2 (20) **(18.4)**	–	–
	2	#1.2 (80) **(83.4)**	#2.3 (20) **(16.6)**	–	–
	3	#1.1 (30) **(56.9)**	#5.3 (70) **(43.1)**	–	–
Three soil samples	4	#4.2 (10) **(20.0)**	#5.3 (80) **(57.3)**	#6.1 (10) **(22.7)**	–
	5	#1.2 (20) **(19.3)**	#3.1 (70) **(74.2)**	#4.3 (10) **(6.6)**	–
	6	#1.1 (30) **(41.5)**	#3.3 (50) **(49.5)**	#5.3 (20) **(9.0)**	–
	7	#2.3 (80) **(74.4)**	#3.1 (10) **(12.9)**	#6.2 (10) **(12.7)**	–
Four soil samples	8	#1.1 (10) **(12.4)**	#2.3 (70) **(62.9)**	#3.1 (10) **(12.5)**	#6.2 (10) **(12.3)**
	9	#1.1 (10) **(10.3)**	#2.3 (10) **(7.4)**	#3.1 (70) **(72.2)**	#6.2 (10) **(10.2)**

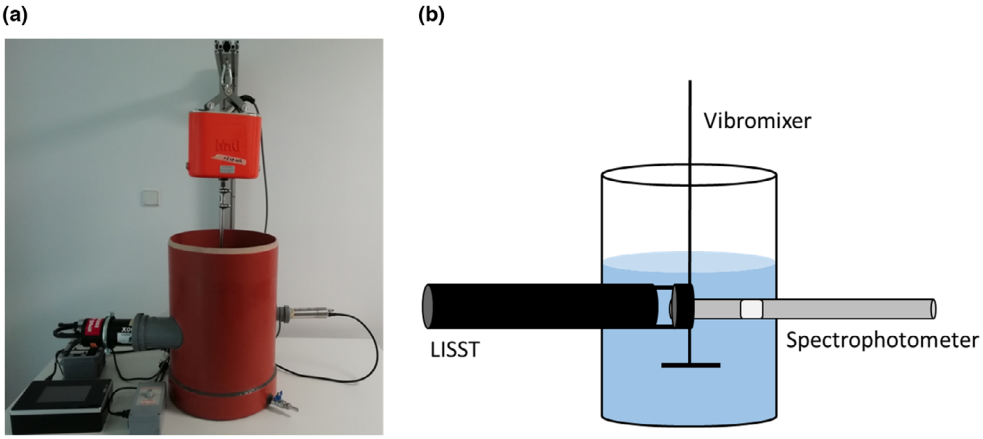

FIGURE 1 Photograph (a), and schematic representation (b) of the laboratory tank set-up. The data obtained from the spectrophotometer are discussed in Lake et al. (2022).

measurements, with percentage of volume concentration being independent from mass concentration.

The LISST sensor was installed in a water tank (75.4 L capacity) filled with 40 L of demineralised water (Figure 1). The sensor was installed in a horizontal orientation to prevent the settling of particles on the sensor lens. The LISST sensor was equipped with the path reduction module to cope with all measured concentrations (Sequoia Scientific, 2018). Both individual soil samples and mixtures were tested for 10 different theoretical concentrations to investigate the influence of different concentrations on the un-mixing results (100–1000 mg L^{-1}, at 100 mg L^{-1} increments). A background signal (using demineralised water), measured before the start of every experiment, was saved onto the instrument and automatically compensated for during the experiments (to eliminate influence on the measurements of e.g., small scratches on the measurement window). For each theoretical concentration, the LISST sensor measured over a 10-min period at 1.5 second interval, using a random shape algorithm (Sequoia Scientific, 2018). After each theoretical concentration was measured, three samples were collected using a pipette. Samples were transferred into pre-weighed aluminium buckets and dried to quantify the concentrations inside the tank (i.e., 'measured concentrations').

A Vibromixer (DrM, Dr. Mueller AG, Switzerland) mixing device was used to keep the soil samples and mixtures in suspension (see Lake et al., 2022 for details on the settings and initial tests on mixing performances). From the results in Lake et al., 2022, it appeared that measured concentrations were lower than the theoretical concentrations, with differences increasing with an increase in particle size. Soil samples sieved to the same size fractions presented similar differences between measured and theoretical concentrations. Since mixtures 1–9 used soil samples sieved to different size fractions, the actual in-tank contributions differed from the theoretical input contributions. Therefore, input contributions for these mixtures were compensated according to the measured soil sample concentrations. Table A.3 shows the measured concentrations and Table 1 the associated compensated soil sample input contributions for the mixtures.

2.2 | Field experiments

The field experiment was carried out at the confluence of a tributary draining a sub-catchment with different underlying geology, which was hypothesized to yield SS with distinct PSDs (as discussed in Walling et al., 2000) compared to the rest of the catchment. Field

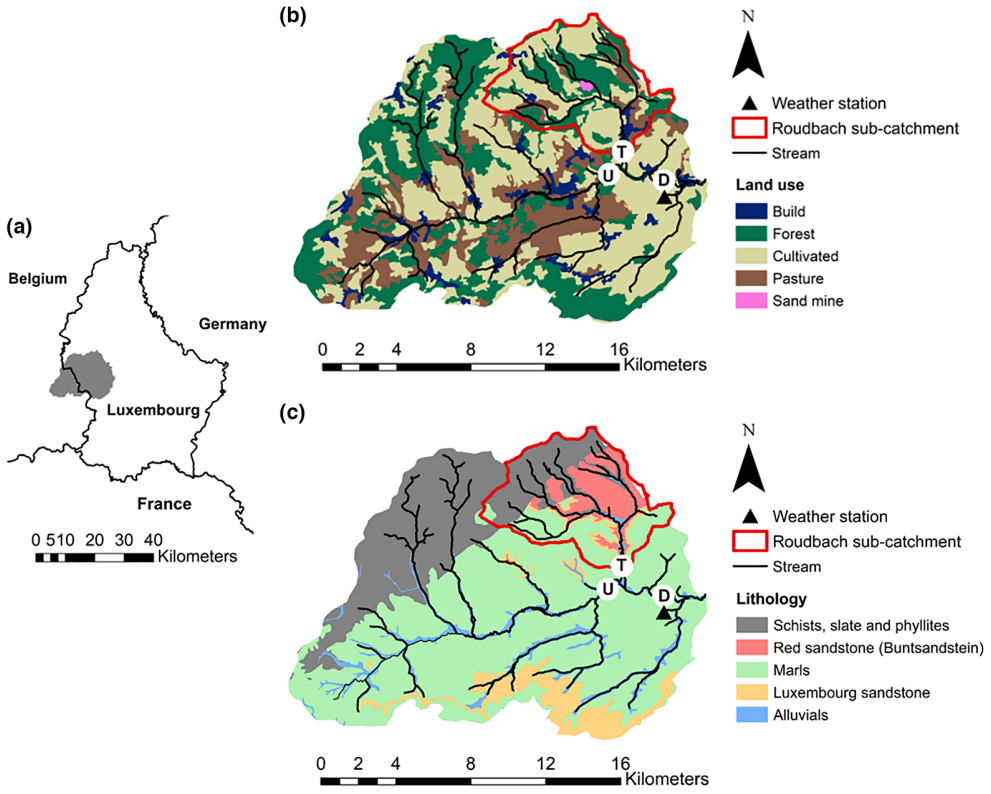

FIGURE 2 Location of the Attert River basin in Luxembourg (a), land use and river network at Useldange (b), and lithology and river network at Useldange (c). Sampling sites (b and c) are indicated by the letters U (upstream), T (tributary), and D (downstream).

samples were collected using automatic water samplers (i.e., discrete samples) at pre-set times at the two upstream and downstream sites. PSDs, measured on the samples were introduced into the grain-size un-mixing model to identify the origin of the downstream target SS. A sediment budget, through a simple mass-balance, was used to evaluate the model results.

2.2.1 | Study area

The study area is located in the Attert River basin (247 km^2 at Useldange), in the western part of Luxembourg (Figure 2a). Land use is represented by forests (dominant in the higher sloping schist and sandstone areas), grasslands and croplands (Figure 2b). The catchment is underlain by schists, slate and phyllites bedrock in the north-west, and by red sandstone ('Buntsandstein'), marls and Luxembourg sandstone in the central and southern parts (Figure 2c). Altitudes range from 553 to 238 m above sea level. The climate is semi-oceanic, with maximum mean monthly temperatures ranging between 0 and 18°C and an average annual rainfall of ~845 mm (1954–1996; Pfister et al., 2005). Precipitation during the field experiments was measured at the weather station in Useldange (Figure 2b,c) by the 'Administration des Services Techniques de l'Agriculture' (ASTA; https://www.agrimeteo.lu).

Three sites were instrumented for stream water sampling (Figure 2b,c). Two sampling sites were located along the Attert River, upstream and downstream of the Roudbach tributary junction. The third sampling site was located at the outlet of the Roudbach tributary. The Roudbach sub-catchment drains an area of 44 km^2 and is mainly underlain by red sandstone ('Buntsandstein'), as well as by schists, slate and phyllites bedrock in the northern part. Discrete water samples were collected during storm runoff events and low flow periods using automatic water samplers (ISCO 6712 FS; Teledyne ISCO, Lincoln, Nebraska, U.S.A). Sampling at the three sites was undertaken at the same time. Until analyses, samples were stored in a cold room (4–5°C). At each of the three sites, turbidity was measured at 5-min intervals using a S::can spectro::lyser™ probe (Scan Messtechnik GmbH, Vienna, Austria).

2.2.2 | Particle size distribution measurements

Particle size distributions of the SS contained within the discrete water samples were measured in the laboratory using a Mastersizer 3000 (Malvern Instruments, Malvern, UK). Discrete samples were shaken for homogenization and a sub-sample was introduced into the Mastersizer hydro LV unit (3000 rpm mixer rotation speed), collecting a total of five measurements per sample. Samples were introduced to the Mastersizer until a certain obscuration range was achieved (usually between 3% and 5%) to allow for consistency between measurements. For samples with low concentrations, this obscuration range was not always achieved. The PSD of each sample was measured after applying ultrasound for 60 seconds to disaggregate potential flocs and to measure the absolute particle size (representing the primary particles; Biggs & Lant, 2000).

Organic matter (OM) was removed from a selection of samples to investigate (i) the influence of OM on the PSD shape, and (ii) to investigate whether PSDs measured from SS with OM removed improved un-mixing accuracy. To this end, a selection ($n = 12$, 4 samples for each site) of discrete samples from period F (Figure 4; Table 2) were oven dried at 35°C. Subsequently, these samples were removed using Milli-Q water and transferred into a glass beaker. Hydrogen peroxide (H_2O_2) was added to these beakers, which were then placed on a hot plate (30–35°C). Samples were stirred and H_2O_2 was added until all OM was removed. Samples were then disaggregated in an ultrasonic bath and subsequently introduced into the Mastersizer.

2.2.3 | Suspended sediment budget

A suspended sediment budget (mass balance) was established to evaluate the un-mixing model performance. To this end, suspended sediment concentration (SSC) was measured from the discrete water samples by filtering a known volume through 1.2 μm Whatman GF/C glass fibre filters. These concentrations were used, together with the in-stream turbidity measurements, to establish a sediment calibration curve for each sampling site (Figure A.1; $r^2 = 0.84$, 0.86 and 0.88 and $n = 126$, 121 and 129 for the Upstream, Tributary and Downstream sites, respectively). Predicted SSCs and discharge data were used to calculate SS loads at 5-min time steps. Total Downstream SS loads, based on the sum of Upstream and Tributary SS loads, were then divided into the relative contributions of both the Upstream and Tributary sites (hereafter referred to as 'sediment budget'). At the Tributary site, turbidity values were not recorded during a 3-hour period due to very high sediment concentrations (04/06/2021 18:00–04/06/2021 21:00). Therefore, SSC predictions during that period were based on a linear interpolation between the available measured SSCs. Downstream discharge was calculated based on the sum of discharges from both the Upstream and Tributary sites (with half an hour delay applied as an estimate of river water travel time).

2.3 | AnalySize modelling

The AnalySize software (version 1.2.1; Paterson & Heslop, 2015) was used to perform the un-mixing of: (i) the artificial laboratory mixtures into the soil samples contributions, and; (ii) the field downstream samples into the contributions of the Upstream and Tributary sources. The AnalySize model was selected based on Van Hateren et al. (2018), wherein the authors compared the performances of different end-member mixing models with decomposed grain-size distribution data using an artificial data set with known source proportions. The authors concluded that the AnalySize algorithm provided the most accurate results. Furthermore, the algorithm allows accounting for the known end-member PSD data (i.e., the Tributary and Upstream sources in this case). AnalySize is a MATLAB based software tool, which is freely available for download (Paterson & Heslop, 2020a), together with a detailed manual (Paterson & Heslop, 2020b).

The AnalySize algorithm is inspired by hyperspectral image analysis (Paterson & Heslop, 2015). Its un-mixing principle is similar to that of mass balance un-mixing models widely used by the sediment fingerprinting community (e.g., Collins et al., 1997b; Lizaga et al., 2020; Pulley & Collins, 2018; Stock et al., 2018), where data that are to be un-mixed can be described as a linear mixture of the contributing end-members. End-member abundance must be >0 and sum to 1 (100%). In the AnalySize algorithm, the PSD data are expressed as relative abundances of each size class and must sum to one. The un-mixing principle (Equation 1) can be expressed in matrix notation (Paterson & Heslop, 2015):

$$X = AS + E, \tag{1}$$

where X is the observed data (PSD of a target SS sample; one specimen per row), A the abundance matrix of the constituent end-members (i.e., relative contribution of each tributary) whose signatures are given by S (PSD of the tributaries; one end-member per row), and sampling and measurement errors are represented by E. As described by Paterson and Heslop (2015), due to the imposed constraints, there is no closed form solution to equation (1), which thereby has to be solved numerically.

Within AnalySize, the target SS PSD data were loaded using the 'Load Data' button. End-member PSDs were entered using the 'Defined' end-member option, as source PSD was measured and could be directly used to determine its abundance. Based on the PSDs of the tributary sources and target SS, AnalySize displays several performance indicators, including EM-r^2 (indicating the maximum squared linear correlation between the end member [EM] PSDs, being a measure of linear independence between the potential sources).

2.3.1 | Un-mixing of artificial laboratory mixtures

The PSDs of the soil samples measured in the tank set-up were used as source data to un-mix the PSDs measured on the artificial mixtures. Source data were created by averaging all recorded PSDs over all concentrations. Mixture PSD data were introduced for each single measurement separately, with AnalySize predicting, for each measurement, the relative abundance of the soil samples mixed in the tank set-up. In the present study, size classes ranging from 1 to 500 μm were included for analysis. Modelled results were compared with the known relative soil sample contributions (section 2.1.2).

2.3.2 | Un-mixing of suspended sediment field samples

For consistency with the laboratory results, the upper size limit for the Mastersizer measurements on the field samples was set to 500 μm. This approach allowed the inclusion of the main PSD peak, while eliminating (smaller) peaks at larger particle size ranges (>500 μm) that were associated with small leaves or coarser particles

TABLE 2 Summary hydro-sedimentological data for the measurement periods

Period	Start - end dates and times	Total precipitation (mm)	Sampling site	Maximum measured SSC (mg L^{-1})	Maximum discharge (m^3 s^{-1})	Total sediment load (t)	Total discharge (mm)
A	10/03/2021 21:00 - 15/03/2021 11:55	30.4	Upstream	535	17.0	250.2	10.6
			Tributary	424	1.5	13.2	6.0
			Downstream	440	18.1	212.4	9.1
B	02/04/2021 14:15 - 09/04/2021 12:00	1.6	Upstream	97	1.2	4.8	3.7
			Tributary	4	0.4	1.1	4.3
			Downstream	3	1.6	11.7	3.7
C	09/04/2021 12:00 – 13/04/2021 13:20	35.1	Upstream	310	7.9	59.6	6.5
			Tributary	155	1.1	8.8	5.0
			Downstream	132	9.0	55.7	5.9
D	10/05/2021 00:00 – 12/05/2021 17:00	4.7	Upstream	17	1.8	1.4	1.4
			Tributary	55	0.4	0.46	1.4
			Downstream	51	2.1	4.48	1.3
E	16/05/2021 00:00 – 18/05/2021 12:00	17.6	Upstream	143	2.2	3.8	2.2
			Tributary	33	0.47	0.94	1.8
			Downstream	24	2.5	4.1	2.0
F	03/06/2021 13:00 – 06/06/2021 01:00	44.2	Upstream	520	6.6	98.7	2.9
			Tributary	2368	1.1	31.4	2.2
			Downstream	455	7.4	102.2	2.6
G	13/07/2021 00:00 – 16/07/2021 12:00	101.5	Upstream	410	69.1	1039.0	35.7
			Tributary	1162	10.1	382.4	22.9
			Downstream	700	79.3	1323.0	31.3

(Figure A.2, Figure A.5). The five PSD measurements per sample were averaged for the source samples; all five individual measurements of the Downstream samples were used in AnalySize.

3 | RESULTS

3.1 | Laboratory experiments: Model evaluation using artificial mixtures

Modelled contributions for the respective soil samples, for mixtures consisting of soil samples sieved to different size fractions, are shown in Figure 3a. Overall, modelled contributions predicted the same dominant soil samples compared with the known input contributions. Differences between averaged modelled contributions and known input contributions to the mixtures were small (Table A.5), with deviations >10% only observed for soil samples in mixtures 3 (14%, for soil samples #1.1 and #5.3), 4 (13%, for soil sample #5.3), 7 (11%, #2.3), 8 (10%, #1.1) and 9 (10%, #1.1).

Mixture 2 differed from the other mixtures in terms of the high standard deviations associated with the modelled contributions (34%), which were < 15% for all other soil samples (Table A.4). For Mixture 2, mixture D_{50} values (Figure A.4) unexpectedly increased with increasing concentrations (up to theoretical concentrations of 600 mg L^{-1}). D_{50} values then returned to their starting values (observed at 100 mg L^{-1}) and remained constant at the higher theoretical concentrations tested (600–1000 mg L^{-1}). Following the patterns observed in the D_{50} values, modelled contributions (Figure A.4) for soil sample #1.2 (83% input contribution) started between 80% and 100%, decreasing in a stepwise manner to ranges of 30%–50%, 10%–30% and 5%–15%. Thereafter, for concentrations exceeding 600 mg L^{-1}, modelled contributions for the soil sample returned to very high values of 90%–100%. Similar stepwise increases of D_{50} values were observed for several other mixtures and/or soil samples

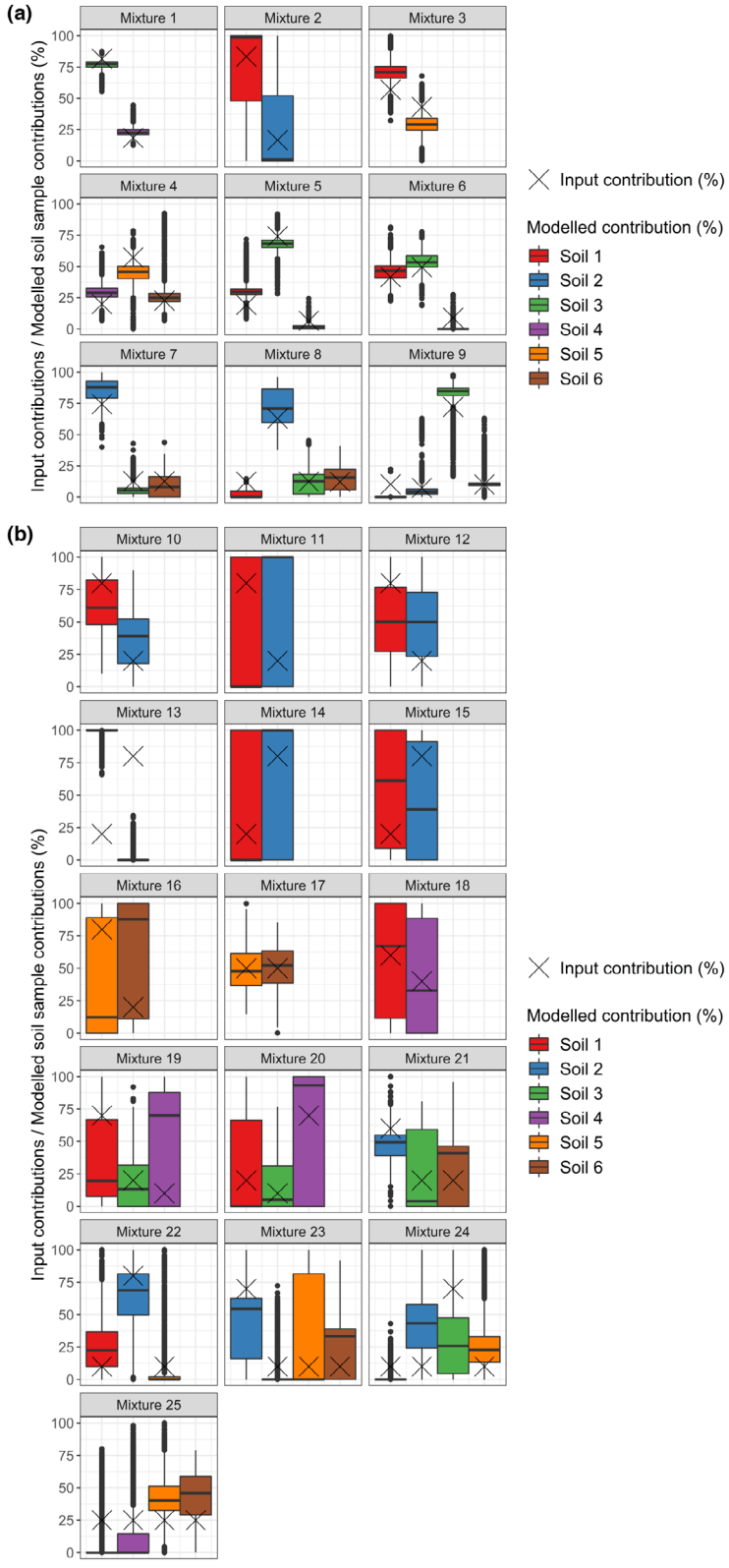

FIGURE 3 Modelled contributions (boxplots, with median shown by central line, interquartile range by box, and range by whiskers) for the laboratory experiments using artificial mixtures consisting of soil samples sieved to different size fractions. These modelled contributions are compared with the known input contributions of soil samples in each of the mixtures (black crosses). Mixtures 1–9 consist of soil samples sieved to different fractions (a). Mixtures 10–25 consist of mixtures sieved to same fractions (b).

(e.g., soil sample #1.2, #3.1, #4.2 and #6.2). These patterns mostly occurred at lower theoretical concentrations (100–500 mg L^{-1}), which caused a spread in the modelled soil sample contributions at these lower concentrations, although to a much smaller extent than observed for mixture 2.

Modelled predictions for the mixtures with soil samples sieved to the same size fractions exhibited larger deviations from the known input contributions (Figure 3b). For those mixtures using four soil samples, several modelled soil sample contributions were estimated at 0%. Only a few modelled soil sample contributions were close to the

known input contributions. This observation was, for example, notable for the soil samples in mixture 17. Particle sizes of the soil samples in mixture 17 were, although sieved to same fractions, significantly different (*t*-test; *p*-value of <0.001) showing a larger difference than the other soil samples sieved to the same size fractions (Figure A.3).

3.2 | Field experiments: Model evaluation using sediment budget estimates

An overview of discharge and precipitation data is shown in Figure 4, with selected periods in which field sampling was performed highlighted. Discharge and precipitation, as well as maximum measured SS concentrations (SSC) during the periods are shown in Table 2. Periods A, C, F and G were high discharge periods, associated with relatively high SSCs. Period B was a discharge recession. Periods D and E were small storm runoff events with measured SSC concentrations lower than during the high discharge periods. During period F, more than 20 mm of rainfall was measured within 2 hours, resulting in a relatively high discharge peak and elevated SSCs (with a maximum of 2368 mg L^{-1}) at the Tributary sampling site (Table 2). Period G was measured during the 2021 extreme flood event in central Europe (14/07/2021–15/07/2021), with a return period of >20 years for the Attert River.

During the storm runoff events, D_{50} values measured on the discrete samples showed an initial increase during the rising limb of the hydrograph and then a decrease before the discharge peak.

Figure 5 presents the modelled predictions using the PSDs measured on the discrete samples to estimate the relative contributions of the Upstream and Tributary sites to the Downstream site. Samples collected at low and mid-flows showed a large variability in modelled contributions (periods A-F); for several cases, contributions reached 100% (and 0%) for both the Upstream and Tributary sites (e.g., periods B, E and F). During storm runoff events (periods A, C and F) the dominant modelled contributions were assigned to the Upstream site directly after the peak discharge. This aligned with the estimated sediment budget contributions, wherein the Upstream site is, in general, the dominant contributor (generally exceeding 60%) to the Downstream target SS. For the large flood event (period G), averaged modelled contributions and estimated contributions from the sediment budget demonstrated relatively small deviations over the whole measurement period (average deviation of 16%, $n = 25$).

There were several observations where increasing contributions from the Tributary, based on sediment budget estimates, coincided with either increasing modelled Tributary contributions or increasing modelling uncertainties. For period C, contributions according to the sediment budget were ~ 50% for both the Upstream and Tributary sources during the steeper rise of the hydrograph (at a discharge of ~4 m^3 s^{-1}). Modelled contributions exhibited large variations around that time, with subsequent contributions for the Tributary source of 1.2%, 86% and 38%. Period F exhibited high variability in modelled source predictions. During the initial stages of the rising limb, this period experienced high sediment loads from the Tributary site (Figure 4 and Table 2). Modelled contributions around that time predicted dominant contributions for the Tributary (with two values predicting a contribution of 100%). During period G, overall discharges were very high and modelled results closely coincided with the source contribution estimates from the sediment budget.. At the peak of the hydrograph and during the falling limb, differences between the sediment budget and modelled contributions were, however, more pronounced (within a 20% range). During the rising limb of the hydrograph in period G, there were three times at which the modelled contributions predicted the Tributary as the dominant source. These results correspond to the variabilities observed in the sediment budget contributions, where the Tributary contributions increased and decreased three times to reach maximum values of 40–45%, and minimum values of ca. 25%, before showing a more stable relative contribution after the peak discharge. Similar patterns were found for period D, where a dominant contribution from the Tributary site was predicted by the model, in agreement with the sediment budget estimates.

3.3 | Field experiments: Relationships between model performance, discharge, source particle size and organic matter content

Model performance improved with increasing discharge (Figure 6a). For discharges <4 m^3 s^{-1}, a wide range of model performances was observed. Above this discharge value, 40 samples out of 46 returned a deviation between modelled and sediment budget-based estimates of <40%, 38 samples <30% and 33 samples <20%. Results (Figure 6) indicate that model performance improved when discharge values exceeded 4 m^3 s^{-1}. Model performance did not improve when there were larger differences in source D_{50} values (Figure 6b) or when OM was removed before PSD measurements (Figure A.5; Table A.6).

4 | DISCUSSION

4.1 | Evaluating model performance using artificial laboratory mixtures

Low absolute errors of 7% ± 4% were observed between the known and modelled contributions for the soil samples sieved to different size fractions (Figure 3a). Lake et al. (2022) reported higher mean absolute errors of 14.5% ± 13.0% when using absorbance as a fingerprint property to model the relative source contributions of the same nine mixtures. Here, our absolute errors between known inputs and modelled outputs are comparable to other studies using artificial mixtures to evaluate un-mixing models, with absolute errors ranging between 10% (Gaspar et al., 2019), 9%–11.8% (Haddadchi et al., 2014) and 11.2% (Pulley et al., 2017). Our results herein thus indicate good accuracy and thus the suitability of the presented modelling approach to estimate the source contributions to the mixtures. On the other hand, our larger mean absolute errors of 22

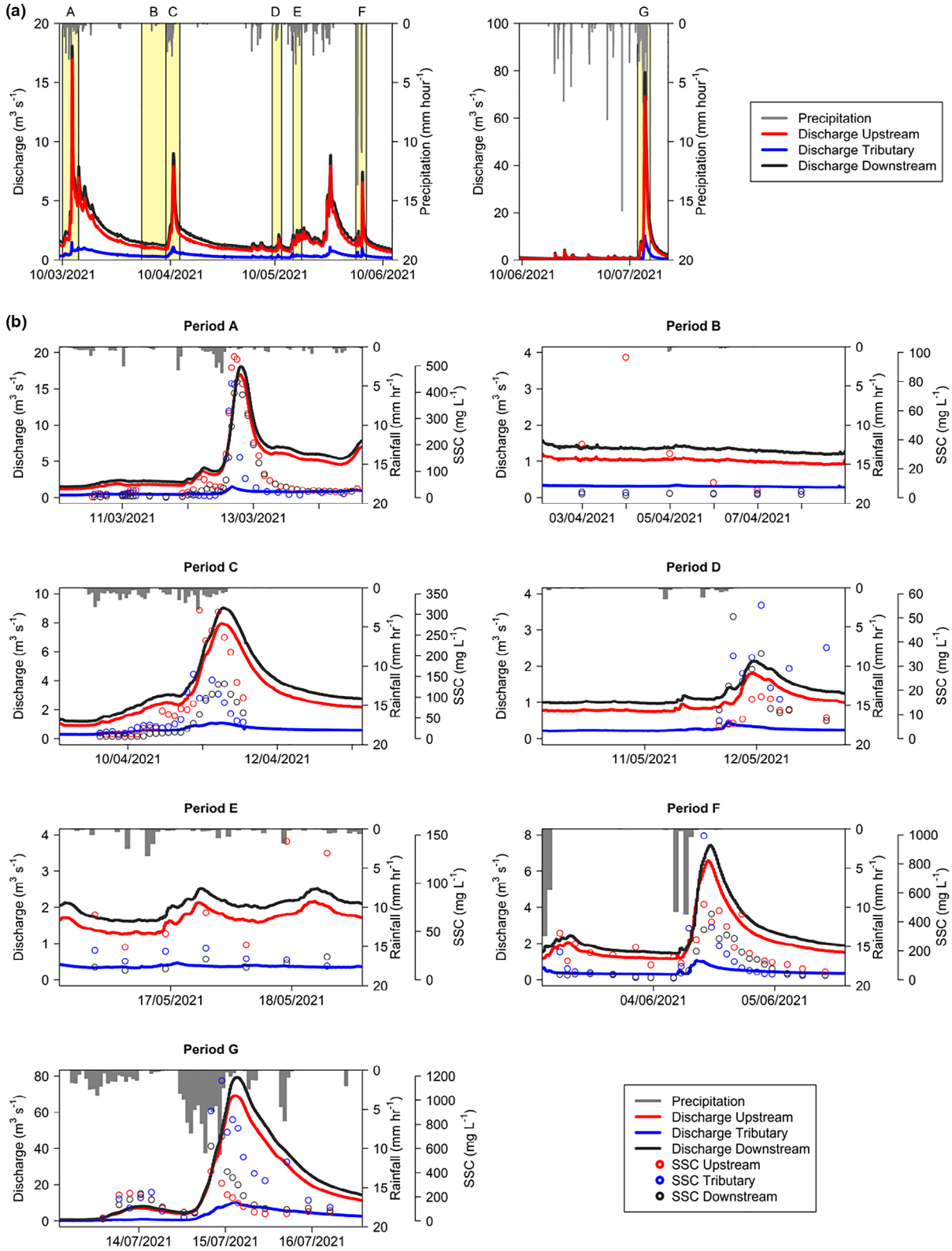

FIGURE 4 Precipitation records from the weather station in Useldange, and discharge records at the three measurement sites. Periods in which field observations were made (A–G) are highlighted in yellow (a). Detail of discharge and precipitation records for the selected periods (A–G), in combination with the measured suspended sediment concentration of the collected samples (b). For period F, the highest value (tributary) is omitted for visual purpose (2367 mg L^{-1}, 04/06/2021 19:30. This value precedes the shown 994 mg L^{-1} value; 04/06/2021 21:00).

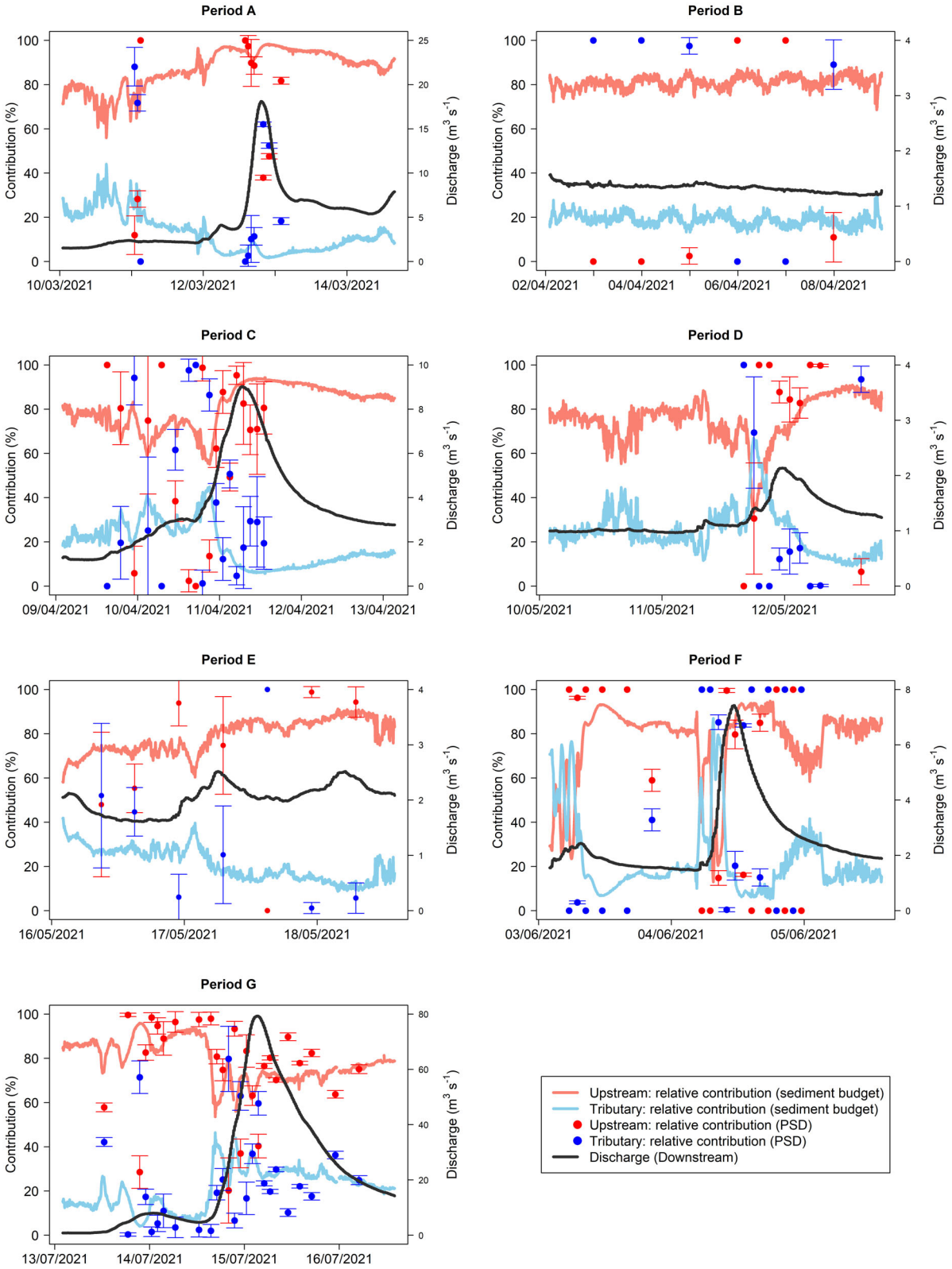

FIGURE 5 Modelled relative contributions of the upstream and tributary sites to the downstream site calculated using PSDs measured on the discrete samples (periods A-G). Modelled contributions are compared with the relative sediment loads (calculated sediment budget) of the upstream and tributary sites (red and blue lines) to the downstream site. Coincidence of dots and lines of similar colour indicates good agreement between the two sets of data. Error bars showing modelled standard deviations

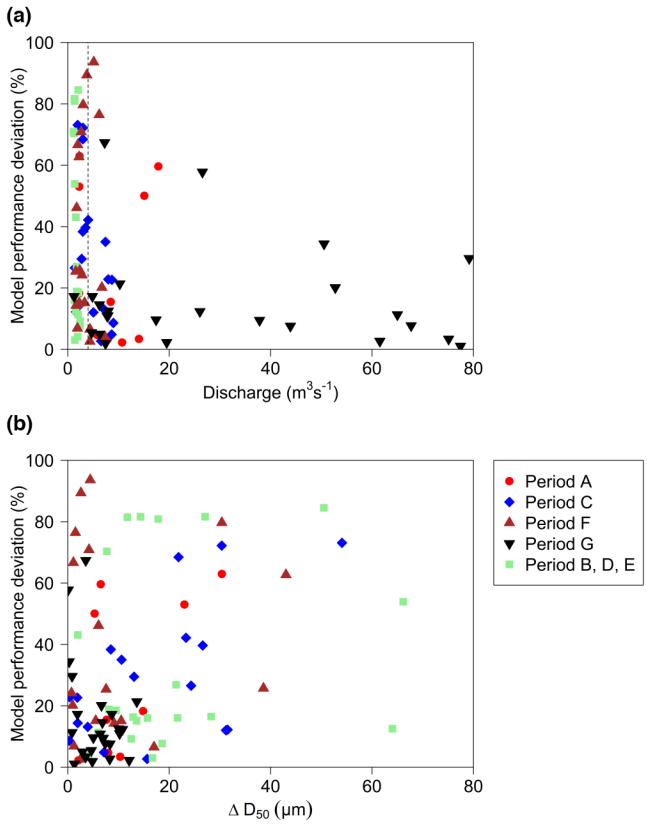

FIGURE 6 Model performance deviation (i.e., absolute difference between the modelling results and the calculated sediment budget) as (a) a function of discharge, and (b) ΔD_{50} (i.e., median particle size differences between both sources). A model performance deviation of 0% indicates no difference between the two sets of data. The discharge threshold values as discussed in the text are shown by a vertical dotted line (discharge: 4 $m^3 s^{-1}$, (a)). Results for the largest events (periods a, C, F and G) are shown individually; smaller events and low flow (periods B, D and E) are shown together.

± 19% when un-mixing the laboratory mixtures consisting of soil samples sieved to the same size fractions ($n = 16$; Figure 3), indicate that smaller differences in PSD and D_{50} between source samples understandably had a negative influence on the accuracy of modelling. This inaccuracy can also be observed in the modelled contributions of either 0% or 100%. This most likely indicates the inability of the model to distinguish between sources that are similar. This limitation has been observed in previous sediment fingerprinting studies (e.g., Cooper et al., 2014) and suggests limitations of the un-mixing model principles.

Particular consideration must be given to the fact that AnalySize predictions were mainly influenced by the measured variability in the PSDs of the mixtures. The soil samples (end-members) PSDs were averaged over all tested concentrations (100–1000 mg L^{-1} range), under the assumption that PSD remained constant during the experiment. However, with the observed variations in soil sample D_{50} values, modelling of each concentration separately would have eventually resulted in larger model inaccuracies. This is pertinent when considering the lower concentrations tested, as the higher variations in D_{50} values were observed in the 100–500 mg L^{-1} range (Figure A.4). Consequently, results for the higher concentrations would in that scenario be more constant and more accurate. Similar observations (i.e., higher inaccuracy at lower concentrations) were reported in Lake et al. (2022).

In contrast to other studies using shear cells to investigate flocculation effects (e.g., Biggs & Lant, 2000, who used activated sludge to analyse floc size in relation to shear), the experiments here did not show signs of floc formation or aggradation inside the tank set-up. This was supported by the continuous LISST measurements (Figure A.4), which showed that D_{50} values varied little (representing the absolute PSD obtained after disaggregation and sieving). Furthermore, SSCs also varied little during the course of the experiments; a constant percentage of added soil sample or mixture material being observed in suspension (see Lake et al., 2022, Figure A.6).

4.2 | Un-mixing field SS samples: Influence of discharge, source particle size, and organic matter content on model performance

The catchment scale field experiments suggested that discharge exerts a strong control on the model performance. Walling et al. (2000) argued that, during the initial phase of storm hydrographs (i.e., rising limb), sediment is transported from a range of different sources, and subsequent changes in particle size could be linked to changes in contributions from those different sources. After these initial sources (e.g., sediment stored on the riverbed) are depleted, however, alternative sources within the catchment can become dominant. This can result in more constant source contributions and thus a more constant texture for sediment in the stream. The latter scenario provides better conditions for making reliable source contribution estimations using PSDs as a fingerprint property. The improved accuracy of sediment fingerprinting estimates during high discharges (>4 $m^3 s^{-1}$) could also be linked to the limited settling, and thereby, improved mixing of sediment being routed through the channel system (Agrawal & Pottsmith, 2000). Discharges exceeding this threshold were observed for 12% of the time (Downstream site) during the study period (Figure 4; 10/03/2021–21/07/2021), with a mean measured discharge during that period of 2.5 $m^3 s^{-1}$. During this 12% of the time, 82% of the total SS load (Downstream site) was transported.

Besides the potential changes in SS source PSDs, different flocculation processes could affect the observed in-stream PSDs (e.g., Droppo, 2004; Grangeon et al., 2014). Suspended sediment floc sizes, in combination with their shape and density, determine the potential of particles to be transported due to their relationship with settling velocity (Williams et al., 2008). This corroborates with our observations that under high-flow conditions, measured PSDs appeared to be more reliable for the use of un-mixing when compared with low-flow conditions. Droppo (2004) argued that the aggregated sizes of SS particles are mostly being controlled by particle concentration and flow shear stress. However, the effect of these dominant in-channel flocculation processes on the measured PSDs (e.g., Grangeon

et al., 2012) was assumed to be rather limited, as settling was assumed to be mostly absent (especially under high-flow conditions). This suggests that most SS material observed at the source sites was transported to the downstream target SS site regardless of any flocculation occurring in between. To account for any of these in-stream flocculation processes between the sites, we hypothesized during this proof-of-concept study that these effects were minimized by measuring and comparing only the sources and downstream absolute PSDs (i.e., primary particles). Thereby, due to the absence of clear erosion or deposition between the source sites and the target SS sampling site (confirmed by visual observations), it was assumed here that the SS transported downstream was a simple sum of the SS from the upstream sources.

An increase in the D_{50} values was observed at the start of the monitored storm events, which could suggest the remobilisation of sediment stored on the riverbed (e.g., Lawler et al., 2006; Walling et al., 2000). Thereafter, D_{50} values decreased, most probably due to the depletion of these sources. Temporal variability in PSDs during events, related to the activation of different sources during the storm hydrograph, has also been observed in other studies (e.g., Grangeon et al., 2012; Slattery & Burt, 1997; Upadhayay et al., 2021; Vale et al., 2020). It is therefore important to have a good estimation of transport times between sampling sites when using PSDs for sediment source fingerprinting. This is to avoid time-related issues in the direct comparison of the PSDs of SS samples collected at different sites. Travel times between measurements points could be subject to change depending on flow conditions. In the present study, samples from the three sites collected at the same time were compared directly (i.e., no adjustment was used for travel times). This is because of the relatively short distances (ca. 3 km), and thus short travel times, from both sources (i.e., Upstream and Tributary sites) to the Downstream sampling site. These decisions might, however, have introduced some uncertainty in the estimated source contributions using the established mass-balance sediment budget.

Previous work has shown that oxidation of organic matter can improve modelling results when fingerprinting SS sources (Pulley & Collins, 2022; Pulley & Rowntree, 2016). In the present study, the organic matter of some samples collected during period F was oxidized to investigate its effect on the PSDs (as discussed by Gray et al., 2010) and subsequent un-mixing results. Removal of the organic matter did not improve un-mixing model accuracies for those samples tested (Figure A.5; Table A.6). However, these results can be important to understand what size fractions in the PSDs were influenced by the OM. This information can then help to eliminate OM effects on the PSD, (>500 μm) to only investigate the primary particles that were hypothesized to better represents the sources.

4.3 | Critical considerations for using particle size data for sediment source fingerprinting

Application of the approach presented herein uses differences in PSDs to discriminate between the sources. A first indication of potential differences in PSDs can be gained by looking at potential contrasts based on geology and soils (Walling et al., 2000), as was undertaken for the field experiment part of this study. This preliminary screening can help to avoid situations in which D_{50} values for different tributaries or soil sources are not sufficiently differentiated (as observed in a recent confluence-based fingerprinting study by Patault et al., 2019). Results presented herein, nonetheless, indicated that to achieve accurate un-mixing results, differences in D_{50} values can be relatively small (Figure 6b). This is also true for period G, with a deviation between the un-mixing results and sediment budget of 16%; that is, the sampling period with the best performing performance. Here differences in source D_{50} values were, on average, only 6 μm.

Similarly, attention should be directed to collecting representative samples. Samples collected at different depths (Bainbridge et al., 2012) or at different distances from the channel bank (Walling et al., 2000) can manifest distinctive SS particle sizes. This latter point relates to our suggestion that for period G, a higher level of turbulence could have resulted in better mixing of the SS in the water column, leading to more representative sampling and more representative PSD data. This situation appeared to improve the un-mixing results, even with the relatively small differences between source D_{50} values. Sampling is also affected by the field equipment used. Field samples were collected using automatic water samplers, for which installation was subject to sampling site limitations. The pumping might, as reported by Grangeon et al. (2012), create a vortex at the inlet opening of the tube that could affect the amount of SS collected and its corresponding particles sizes. This issue highlights the potential uncertainties associated with the automatic samplers deployed.

To analyse particle size, different instruments are available (herein we presented the use of two instruments: the LISST and Mastersizer). As results may differ depending on the type of equipment used (Bieganowski et al., 2018), we recommend that due care and attention are exercised when PSDs or D_{50} values are compared both within and between studies. Furthermore, many different measurement protocols were found in existing literature that can affect measurements, including different machine settings (e.g, rotating stirrer speed), sample preparations (treatment with dispersive agent, duration of ultrasound) and sampling collections (number of measurements) (e.g., Cooper et al., 2014; Dietze et al., 2012; García-Comendador et al., 2021; Grangeon et al., 2012; Patault et al., 2019; Pulley et al., 2018, 2017). Therefore, in the absence of a standard protocol to measure PSDs, it is a good practise to use the same equipment and apply similar measurement protocols when aiming to compare PSD data directly (Bieganowski et al., 2018).

Sediment source fingerprinting results using PSD data could also be compared with un-mixing results using conventional fingerprinting properties and one of the current un-mixing models used by the international scientific community. This would allow some degree of independent validation of PSDs as a fingerprint. The independent validation of sediment source fingerprinting estimates has been rarely undertaken (e.g., Batista et al., 2022; Gaspar et al., 2019). To validate

estimated source proportions using PSDs as a fingerprint herein, we used sediment budget estimates generated using conventional water sampling; this has, to date, been used in few sediment fingerprinting studies (e.g., Collins et al., 1998; Dabrin et al., 2021; Tiecher et al., 2022), mainly due to the extra costs associated with the installation of equipment and sampling (Collins et al., 2020, 2017; Collins & Walling, 2004).

5 | CONCLUSIONS

In this research, the use of PSDs to fingerprint suspended sediment sources was tested at laboratory and catchment scales. To this end, we used an end-member grain size un-mixing modelling algorithm (AnalySize). The laboratory tests, using mixtures with soil samples sieved to different size fractions, resulted in accurate un-mixing results for the two, three and four soil samples mixtures tested. Observed absolute errors (7 ± 4%) were found to be in the same range or even smaller compared with other research using artificial mixtures to evaluate un-mixing model accuracy. Field data were collected using a confluence-based approach, with relatively short distances (ca. 3 km) between the source sampling sites and the target SS sampling site. The corresponding un-mixing results were more accurate at higher discharges (with an average deviation of 19% from the estimated sediment budget, for discharges >4 $m^3 s^{-1}$). The approach described herein, using PSDs in combination with a grain-size un-mixing model, could support the growing sediment fingerprinting community with an additional fingerprint that is relatively easy to obtain. This is especially of merit since PSD measurements are already routinely made in many sediment source fingerprinting studies.

ACKNOWLEDGEMENTS

Discharge data for the Attert at Reichlange (Upstream site) was generated by the Luxembourg water agency (Administration de la Gestion de l'Eau). The discharge data for the Tributary and Downstream sampling sites was generated by the 'Observatory for Climate, Environment & Biodiversity' of LIST. We would like to thank Dhruv Sehgal for his help in designing the tank set-up and for the discussions during the laboratory experiments. We thank François Barnich for constructing the laboratory tank set-up, and Viola Huck and Jean-François Iffly for their help in instrumenting and maintaining the field sites.

FUNDING INFORMATION

This research was funded by the Luxembourg National Research Fund (FNR) (PAINLESS project; C17/SR/11699372). The contribution to this paper by ALC was funded by UKRI-BBSRC (UK Research and Innovation - Biotechnology and Biological Sciences Research Council) grant BBS/E/C/000I0330.

DATA AVAILABILITY STATEMENT

Particle size distribution data from both the laboratory experiments and the field samples are available at zenodo.org (Lake & Martínez-Carreras 2022, https://doi.org/10.5281/zenodo.7139557). For more information please contact the authors (Niels Lake, niels.lake@list.lu; Nuria Martinez-Carreras, nuria.martinez@list.lu).

ORCID

Niels F. Lake https://orcid.org/0000-0002-5909-2005

REFERENCES

Agrawal, Y. C., & Pottsmith, H. C. (2000). Instruments for particle size and settling velocity observations in sediment transport. *Marine Geology*, *168*, 89–114. https://doi.org/10.1016/S0025-3227(00)00044-X

Bainbridge, Z. T., Wolanski, E., Álvarez-Romero, J. G., Lewis, S. E., & Brodie, J. E. (2012). Fine sediment and nutrient dynamics related to particle size and floc formation in a Burdekin River flood plume, Australia. *Marine Pollution Bulletin*, *65*, 236–248. https://doi.org/10.1016/j.marpolbul.2012.01.043

Batista, P. V. G., Laceby, J. P., & Evrard, O. (2022). How to evaluate sediment fingerprinting source apportionments. *Journal of Soils and Sediments*, *22*, 1315–1328. https://doi.org/10.1007/s11368-022-03157-4

Belmont, P., Gran, K. B., Schottler, S. P., Wilcock, P. R., Day, S. S., Jennings, C., Lauer, J. W., Viparelli, E., Willenbring, J. K., Engstrom, D. R., & Parker, G. (2011). Large shift in source of fine sediment in the upper Mississippi River. *Environmental Science & Technology*, *45*, 8804–8810. https://doi.org/10.1021/es2019109

Beuscher, S., Krüger, S., Ehrmann, W., Schmiedl, G., Milker, Y., Arz, H., & Schulz, H. (2017). End-member modelling as a tool for climate reconstruction — An eastern Mediterranean case study. *PLoS One*, *12*, 1–22. https://doi.org/10.1371/journal.pone.0185136

Bieganowski, A., Ryżak, M., Sochan, A., Barna, G., Hernádi, H., Beczek, M., Polakowski, C., & Makó, A. (2018). Laser Diffractometry in the measurements of soil and sediment particle size distribution. *Advances in Agronomy*, *151*, 215–279. https://doi.org/10.1016/bs.agron.2018.04.003

Biggs, C. A., & Lant, P. A. (2000). Activated sludge flocculation: On-line determination of floc size and the effect of shear. *Water Research*, *34*, 2542–2550. https://doi.org/10.1016/S0043-1354(99)00431-5

Blake, W. H., Ficken, K. J., Taylor, P., Russell, M. A., & Walling, D. E. (2012). Tracing crop-specific sediment sources in agricultural catchments. *Geomorphology*, *139–140*, 322–329. https://doi.org/10.1016/j.geomorph.2011.10.036

Collins, A. L., & Walling, D. E. (2004). Documenting catchment suspended sediment sources: Problems, approaches and prospects. *Progress in Physical Geography: Earth and Environment*, *28*, 159–196. https://doi.org/10.1191/0309133304pp409ra

Collins, A. L., Blackwell, M., Boeckx, P., Chivers, C. A., Emelko, M., Evrard, O., Foster, I., Gellis, A., Gholami, H., Granger, S., Harris, P., Horowitz, A. J., Laceby, J. P., Martinez-Carreras, N., Minella, J., Mol, L., Nosrati, K., Pulley, S., Silins, U., … Zhang, Y. (2020). Sediment source fingerprinting: Benchmarking recent outputs, remaining challenges and emerging themes. *Journal of Soils and Sediments*, *20*, 4160–4193. https://doi.org/10.1007/s11368-020-02755-4

Collins, A. L., Pulley, S., Foster, I. D. L., Gellis, A., Porto, P., & Horowitz, A. J. (2017). Sediment source fingerprinting as an aid to catchment management: A review of the current state of knowledge and a methodological decision-tree for end-users. *Journal of Environmental Management*, *194*, 86–108. https://doi.org/10.1016/j.jenvman.2016.09.075

Collins, A. L., Walling, D. E., & Leeks, G. J. L. (1997a). Use of the geochemical record preserved in floodplain deposits to reconstruct recent changes in river basin sediment sources. *Geomorphology*, *19*, 151–167. https://doi.org/10.1016/s0169-555x(96)00044-x

Collins, A. L., Walling, D. E., & Leeks, G. J. L. (1997b). Source type ascription for fluvial suspended sediment based on a quantitative composite

fingerprinting technique. *Catena*, *29*, 1–27. https://doi.org/10.1016/S0341-8162(96)00064-1

Collins, A. L., Walling, D. E., & Leeks, G. J. L. (1997c). Fingerprinting the origin of fluvial suspended sediment in larger river basins: Combining assessment of spatial provenance and source type. *Geografiska Annaler Series A Physical Geography*, *79*, 239–254. https://doi.org/10.1111/j.0435-3676.1997.00020.x

Collins, A. L., Walling, D. E., & Leeks, G. J. L. (1998). Use of composite fingerprints to determine the provenance of the contemporary suspended sediment load transported by rivers. *Earth Surface Processes and Landforms*, *23*, 31–52. https://doi.org/10.1002/(SICI)1096-9837(199801)23:1<31::AID-ESP816>3.0.CO;2-Z

Collins, A. L., Walling, D., & Leeks, G. J. L. (1996). Composite fingerprinting of the spatial source of fluvial suspended sediment: A case study of the Exe and Severn river basins, United Kingdom. *The journal Géomorphologie: Relief, Processus, Environnement*, *2*, 41–53. https://doi.org/10.3406/morfo.1996.877

Cooper, R. J., Krueger, T., Hiscock, K. M., & Rawlins, B. G. (2014). Sensitivity of fluvial sediment source apportionment to mixing model assumptions: A Bayesian model comparison. *Water Resources Research*, *50*, 9031–9047. https://doi.org/10.1002/2014WR016194

Cooper, R. J., Rawlins, B. G., Lézé, B., Krueger, T., & Hiscock, K. M. (2014). Combining two filter paper-based analytical methods to monitor temporal variations in the geochemical properties of fluvial suspended particulate matter. *Hydrological Processes*, *28*, 4042–4056. https://doi.org/10.1002/hyp.9945

Czuba, J. A., Straub, T. D., Curran, C. A., Landers, M. N., & Domanski, M. M. (2015). Comparison of fluvial suspended-sediment concentrations and particle-size distributions measured with in-stream laser diffraction and in physical samples. *Water Resources Research*, *51*, 320–340. https://doi.org/10.1002/2014wr015697

Dabrin, A., Bégorre, C., Bretier, M., Dugué, V., Masson, M., le Bescond, C., le Coz, J., & Coquery, M. (2021). Reactivity of particulate element concentrations: Apportionment assessment of suspended particulate matter sources in the upper Rhône River, France. *The Journal of Soils and Sediments*, *21*, 1256–1274. https://doi.org/10.1007/s11368-020-02856-0

Dietze, E., Hartmann, K., Diekmann, B., IJmker, J., Lehmkuhl, F., Opitz, S., Stauch, G., Wünnemann, B., & Borchers, A. (2012). An end-member algorithm for deciphering modern detrital processes from Lake sediments of Lake Donggi Cona, NE Tibetan plateau, China. *Sedimentary Geology*, *243–244*, 169–180. https://doi.org/10.1016/j.sedgeo.2011.09.014

Droppo, I. G. (2004). Structural controls on floc strength and transport. *Canadian Journal of Civil Engineering*, *31*, 569–578. https://doi.org/10.1139/L04-015

Droppo, I. G., Nackaerts, K., Walling, D. E., & Williams, N. (2005). Can flocs and water stable soil aggregates be differentiated within fluvial systems? *Catena*, *60*, 1–18. https://doi.org/10.1016/j.catena.2004.11.002

García-Comendador, J., Martínez-Carreras, N., Fortesa, J., Company, J., Borràs, A., & Estrany, J. (2021). Combining sediment fingerprinting and hydro-sedimentary monitoring to assess suspended sediment provenance in a mid-mountainous Mediterranean catchment. *Journal of Environmental Management*, *299*, 113593. https://doi.org/10.1016/j.jenvman.2021.113593

Gaspar, L., Blake, W. H., Lizaga, I., Latorre, B., & Navas, A. (2022). Particle size effect on geochemical composition of experimental soil mixtures relevant for unmixing modelling. *Geomorphology*, *403*, 108178. https://doi.org/10.1016/j.geomorph.2022.108178

Gaspar, L., Blake, W. H., Smith, H. G., Lizaga, I., & Navas, A. (2019). Testing the sensitivity of a multivariate mixing model using geochemical fingerprints with artificial mixtures. *Geoderma*, *337*, 498–510. https://doi.org/10.1016/j.geoderma.2018.10.005

Grangeon, T., Droppo, I. G., Legout, C., & Esteves, M. (2014). From soil aggregates to riverine flocs: A laboratory experiment assessing the respective effects of soil type and flow shear stress on particles characteristics. *Hydrological Processes*, *28*, 4141–4155. https://doi.org/10.1002/hyp.9929

Grangeon, T., Legout, C., Esteves, M., Gratiot, N., & Navratil, O. (2012). Variability of the particle size of suspended sediment during highly concentrated flood events in a small mountainous catchment. *Journal of Soils and Sediments*, *12*, 1549–1558. https://doi.org/10.1007/s11368-012-0562-5

Gray, A. B., Pasternack, G. B., & Watson, E. B. (2010). Hydrogen peroxide treatment effects on the particle size distribution of alluvial and marsh sediments. *Holocene*, *20*, 293–301. https://doi.org/10.1177/0959683609350390

Haddadchi, A., Olley, J., & Laceby, P. (2014). Accuracy of mixing models in predicting sediment source contributions. *Science of the Total Environment*, *497–498*, 139–152. https://doi.org/10.1016/j.scitotenv.2014.07.105

Haddadchi, A., Ryder, D. S., Evrard, O., & Olley, J. (2013). Sediment fingerprinting in fluvial systems: Review of tracers, sediment sources and mixing models. *International Journal of Sediment Research*, *28*, 560–578. https://doi.org/10.1016/S1001-6279(14)60013-5

Hatfield, R. G., & Maher, B. A. (2009). Fingerprinting upland sediment sources: Particle size-specific magnetic linkages between soils, lake sediments and suspended sediments. *Earth Surface Processes and Landforms*, *34*, 1359–1373. https://doi.org/10.1002/esp.1824

He, Q., & Walling, D. E. (1996). Interpreting particle size effects in the adsorption of 137Cs and unsupported 210Pb by mineral soils and sediments. *Journal of Environmental Radioactivity*, *30*, 117–137. https://doi.org/10.1016/0265-931X(96)89275-7

Heslop, D., von Dobeneck, T., & Höcker, M. (2007). Using non-negative matrix factorization in the "unmixing" of diffuse reflectance spectra. *Marine Geology*, *241*, 63–78. https://doi.org/10.1016/j.margeo.2007.03.004

Horowitz, A. J. (1991). *A primer on sediment-trace element chemistry*. Chelsea Lewis Publishing.

Horowitz, A. J., & Elrick, K. A. (1987). The relation of stream sediment surface area, grain size and composition to trace element chemistry. *Applied Geochemistry*, *2*, 437–451. https://doi.org/10.1016/0883-2927(87)90027-8

Koiter, A. J., Owens, P. N., Petticrew, E. L., & Lobb, D. A. (2013). The behavioural characteristics of sediment properties and their implications for sediment fingerprinting as an approach for identifying sediment sources in river basins. *Earth-Science Reviews*, *125*, 24–42. https://doi.org/10.1016/j.earscirev.2013.05.009

Koiter, A. J., Owens, P. N., Petticrew, E. L., & Lobb, D. A. (2018). Assessment of particle size and organic matter correction factors in sediment source fingerprinting investigations: An example of two contrasting watersheds in Canada. *Geoderma*, *325*, 195–207. https://doi.org/10.1016/j.geoderma.2018.02.044

Kranck, K., & Milligan, T. G. (1985). Origin of grain size spectra of suspension deposited sediment. *Geo-Marine Letters*, *5*, 61–66.

Laceby, J. P., Evrard, O., Smith, H. G., Blake, W. H., Olley, J. M., Minella, J. P. G., & Owens, P. N. (2017). The challenges and opportunities of addressing particle size effects in sediment source fingerprinting: A review. *Earth-Science Reviews*, *169*, 85–103. https://doi.org/10.1016/j.earscirev.2017.04.009

Lake, N. F., Martínez-Carreras, N., Shaw, P. J., & Collins, A. L. (2022a). High frequency un-mixing of soil samples using a submerged spectrophotometer in a laboratory setting—Implications for sediment fingerprinting. *Journal of Soils and Sediments*, *22*, 348–364. https://doi.org/10.1007/s11368-021-03107-6

Lake, N. F., & Martínez-Carreras, N. (2022). Data to reproduce the results presented in Lake et al. 2022. Zenodo, Version 1. https://doi.org/10.5281/zenodo.7139557

Lawler, D. M., Petts, G. E., Foster, I. D. L., & Harper, S. (2006). Turbidity dynamics during spring storm events in an urban headwater river system: The upper tame, west midlands, UK. *Science of the Total Environment*, *360*, 109–126. https://doi.org/10.1016/j.scitotenv.2005.08.032

Legout, C., Freche, G., Biron, R., Esteves, M., Navratil, O., Nord, G., Uber, M., Grangeon, T., Hachgenei, N., Boudevillain, B., Voiron, C., & Spadini, L. (2021). A critical zone observatory dedicated to suspended sediment transport: The meso-scale Galabre catchment (southern French Alps). *Hydrological Processes*, *35*, 1–6. https://doi.org/10.1002/hyp.14084

Legout, C., Poulenard, J., Nemery, J., Navratil, O., Grangeon, T., Evrard, O., & Esteves, M. (2013). Quantifying suspended sediment sources during runoff events in headwater catchments using spectrocolorimetry. *Journal of Soils and Sediments*, *13*, 1478–1492. https://doi.org/10.1007/s11368-013-0728-9

Li, Z., Xu, X., Zhang, Y., & Wang, K. (2020). Fingerprinting sediment sources in a typical karst catchment of Southwest China. *International Soil and Water Conservation Research*, *8*, 277–285. https://doi.org/10.1016/j.iswcr.2020.06.005

Liu, C., Lobb, D., Li, S., Owens, P., & Kuzyk, Z. (2014). Using sediment particle size distribution to evaluate sediment sources in the Tobacco Creek watershed. *Geophysical Research Abstracts*.

Lizaga, I., Latorre, B., Gaspar, L., & Navas, A. (2020). FingerPro: An R package for tracking the provenance of sediment. *Water Resources Management*, *34*, 3879–3894. https://doi.org/10.1007/s11269-020-02650-0

Martínez-Carreras, N., Krein, A., Gallart, F., Iffly, J. F., Pfister, L., Hoffmann, L., & Owens, P. N. (2010). Assessment of different colour parameters for discriminating potential suspended sediment sources and provenance: A multi-scale study in Luxembourg. *Geomorphology*, *118*, 118–129. https://doi.org/10.1016/j.geomorph.2009.12.013

Motha, J. A., Wallbrink, P. J., Hairsine, P. B., & Grayson, R. B. (2002). Tracer properties of eroded sediment and source material. *Hydrological Processes*, *16*, 1983–2000. https://doi.org/10.1002/hyp.397

Nosrati, K., Collins, A. L., & Madankan, M. (2018). Fingerprinting sub-basin spatial sediment sources using different multivariate statistical techniques and the modified MixSIR model. *Catena*, *164*, 32–43. https://doi.org/10.1016/j.catena.2018.01.003

Nosrati, K., Fathi, Z., & Collins, A. L. (2019). Fingerprinting sub-basin spatial suspended sediment sources by combining geochemical tracers and weathering indices. *Environmental Science and Pollution Research*, *26*, 28401–28414. https://doi.org/10.1007/s11356-019-06024-x

Oldfield, F., Maher, B. A., Donoghue, J., & Pierce, J. (1985). Particle-size related, mineral magnetic source sediment linkages in the Rhode River catchment, Marylands, USA. *Journal of the Geological Society*, *142*, 1035–1046. https://doi.org/10.1144/gsjgs.142.6.1035

Owens, P. N., Blake, W. H., Gaspar, L., Gateuille, D., Koiter, A. J., Lobb, D. A., Petticrew, E. L., Reiffarth, D. G., Smith, H. G., & Woodward, J. C. (2016). Fingerprinting and tracing the sources of soils and sediments: Earth and ocean science, geoarchaeological, forensic, and human health applications. *Earth-Science Reviews*, *162*, 1–23. https://doi.org/10.1016/j.earscirev.2016.08.012

Patault, E., Alary, C., Franke, C., & Abriak, N. E. (2019). Quantification of tributaries contributions using a confluence-based sediment fingerprinting approach in the Canche river watershed (France). *Science of the Total Environment*, *668*, 457–469. https://doi.org/10.1016/j.scitotenv.2019.02.458

Paterson, G. A., & Heslop, D. (2015). New methods for unmixing sediment grain size data. *Geochemistry, Geophysics, Geosystems*, *16*, 4494–4506. https://doi.org/10.1002/2015GC006070.Received

Paterson, G.A., Heslop, D., 2020a. AnalySize Algorithm. Version 1.2.1. https://github.com/greigpaterson/AnalySize.

Paterson, G.A., Heslop, D., 2020b. AnalySize Manual. Version 1.2.1. https://github.com/greigpaterson/AnalySize/blob/master/Documents/AnalySize_Manual_v1.2.1.pdf.

Pfister, L., Wagner, C., Vansuypeene, E., Drogue, G., Hoffmann, L., Ries, C., 2005. Atlas Climatique du Grand-Duché de Luxembourg. Musée national d'histoire naturelle, Société des naturalistes luxembourgeois, Centre de Recherce Public-Gabriel Lippmann, Administration des services techniques de l'agriculture, Luxembourg, 80.

Pulley, S., & Collins, A. L. (2018). Tracing catchment fine sediment sources using the new SIFT (SedIment fingerprinting tool) open source software. *Science of the Total Environment*, *635*, 838–858. https://doi.org/10.1016/j.scitotenv.2018.04.126

Pulley, S., & Collins, A. L. (2021). The potential for colour to provide a robust alternative to high-cost sediment source fingerprinting: Assessment using eight catchments in England. *Science of the Total Environment*, *792*, 148416. https://doi.org/10.1016/j.scitotenv.2021.148416

Pulley, S., & Collins, A. L. (2022). A rapid and inexpensive colour-based sediment tracing method incorporating hydrogen peroxide sample treatment as an alternative to quantitative source fingerprinting for catchment management. *Journal of Environmental Management*, *311*, 114780. https://doi.org/10.1016/j.jenvman.2022.114780

Pulley, S., & Rowntree, K. (2016). The use of an ordinary colour scanner to fingerprint sediment sources in the south African Karoo. *Journal of Environmental Management*, *165*, 253–262. https://doi.org/10.1016/j.jenvman.2015.09.037

Pulley, S., Foster, I., & Collins, A. L. (2017). The impact of catchment source group classification on the accuracy of sediment fingerprinting outputs. *Journal of Environmental Management*, *194*, 16–26. https://doi.org/10.1016/j.jenvman.2016.04.048

Pulley, S., van der Waal, B., Rowntree, K., & Collins, A. L. (2018). Colour as reliable tracer to identify the sources of historically deposited flood bench sediment in the Transkei, South Africa: A comparison with mineral magnetic tracers before and after hydrogen peroxide pre-treatment. *Catena*, *160*, 242–251. https://doi.org/10.1016/j.catena.2017.09.018

Revel-Rolland, M., Arnaud, F., Chapron, E., Desmet, M., Givelet, N., Alibert, C., & McCulloch, M. (2005). Sr and Nd isotopes as tracers of clastic sources in Lake Le Bourget sediment (NW Alps, France) during the little ice age: Palaeohydrology implications. *Chemical Geology*, *224*, 183–200. https://doi.org/10.1016/j.chemgeo.2005.04.014

Russell, M. A., Walling, D. E., & Hodgkinson, R. A. (2001). Suspended sediment sources in two small lowland agricultural catchments in the UK. *Journal of Hydrology*, *252*, 1–24. https://doi.org/10.1016/S0022-1694(01)00388-2

Sequoia Scientific, I., 2018. LISST-200X Users Manual.

Slattery, M. C., & Burt, T. P. (1997). Particle size characteristics of suspended sediment in hillslope runoff and stream flow. *Earth Surface Processes and Landforms*, *22*, 705–719. https://doi.org/10.1002/(SICI)1096-9837(199708)22:8<705::AID-ESP739>3.0.CO;2-6

Smith, H. G., & Blake, W. H. (2014). Sediment fingerprinting in agricultural catchments: A critical re-examination of source discrimination and data corrections. *Geomorphology*, *204*, 177–191. https://doi.org/10.1016/j.geomorph.2013.08.003

Stock, B. C., Jackson, A. L., Ward, E. J., Parnell, A. C., Phillips, D. L., & Semmens, B. X. (2018). Analyzing mixing systems using a new generation of Bayesian tracer mixing models. *PeerJ*, *6*, e5096. https://doi.org/10.7717/peerj.5096

Stock, B. C., Semmens, B. X. (2016). MixSIAR GUI User Manual. Version 3.1. https://github.com/brianstock/MixSIAR.

Tang, Q., Collins, A. L., Wen, A., He, X., Bao, Y., Yan, D., Long, Y., & Zhang, Y. (2018). Particle size differentiation explains flow regulation controls on sediment sorting in the water-level fluctuation zone of the three gorges reservoir, China. *Science of the Total Environment*, *633*, 1114–1125. https://doi.org/10.1016/j.scitotenv.2018.03.258

Tiecher, T., Ramon, R., de Andrade, L. C., Camargo, F. A. O., Evrard, O., Minella, J. P. G., Laceby, J. P., Bortoluzzi, E. C., Merten, G. H., Rheinheimer, D. S., Walling, D. E., & Barros, C. A. P. (2022). Tributary contributions to sediment deposited in the Jacuí Delta, Southern

Brazil. *Journal of Great Lakes Research*, *48*, 669-685. https://doi.org/10.1016/j.jglr.2022.02.006

Upadhayay, H. R., Granger, S. J., & Collins, A. L. (2021). Dynamics of fluvial hydro-sedimentological, nutrient, particulate organic matter and effective particle size responses during the U.K. extreme wet winter of 2019–2020. *Science of the Total Environment*, *774*, 145722. https://doi.org/10.1016/j.scitotenv.2021.145722

Upadhayay, H. R., Zhang, Y., Granger, S. J., Micale, M., & Collins, A. L. (2022). Prolonged heavy rainfall and land use drive catchment sediment source dynamics: Appraisal using multiple biotracers. *Water Research*, *216*, 118348. https://doi.org/10.1016/j.watres.2022.118348

Vale, S. S., Fuller, I. C., Procter, J. N., Basher, L. R., & Dymond, J. R. (2020). Storm event sediment fingerprinting for temporal and spatial sediment source tracing. *Hydrological Processes*, *34*, 3370–3386. https://doi.org/10.1002/hyp.13801

Vale, S. S., Fuller, I. C., Procter, J. N., Basher, L. R., & Smith, I. E. (2016). Application of a confluence-based sediment-fingerprinting approach to a dynamic sedimentary catchment, New Zealand. *Hydrological Processes*, *30*, 812–829. https://doi.org/10.1002/hyp.10611

van Hateren, J. A., Prins, M. A., & van Balen, R. T. (2018). On the genetically meaningful decomposition of grain-size distributions: A comparison of different end-member modelling algorithms. *Sedimentary Geology*, *375*, 49–71. https://doi.org/10.1016/j.sedgeo.2017.12.003

Wallbrink, P. J., Murray, A. S., Olley, J. M., & Olive, L. J. (1998). Determining sources and transit times of suspended sediment in the Murrumbidgee River, New South Wales, Australia, using fallout 137Cs and 210Pb. *Water Resources Research*, *34*, 879–887.

Walling, D. E., Owens, P. N., Waterfall, B. D., Leeks, G. J. L., & Wass, P. D. (2000). The particle size characteristics of fluvial suspended sediment in the Humber and tweed catchments, UK. *Science of the Total Environment*, *251–252*, 205–222. https://doi.org/10.1016/S0048-9697(00)00384-3

Walling, D. E., Woodward, J. C., & Nicholas, A. P. (1993). A multi-parameter approach to fingerprinting suspended-sediment sources. *Tracers Hydrology*, *1993*, 329–338.

Weltje, G. J. (1997). End-member modeling of compositional data: Numerical-statistical algorithms for solving the explicit mixing problem. *Mathematical Geology*, *29*, 503–549. https://doi.org/10.1007/bf02775085

Williams, N. D., Walling, D. E., & Leeks, G. J. L. (2008). An analysis of the factors contributing to the settling potential of fine fluvial sediment. *Hydrological Processes*, *22*, 4153–4162. https://doi.org/10.1002/hyp.7015

Wynn, J. G., Bird, M. I., & Wong, V. N. L. (2005). Rayleigh distillation and the depth profile of 13C/ 12C ratios of soil organic carbon from soils of disparate texture in iron range National Park, far North Queensland, Australia. *Geochimica et Cosmochimica Acta*, *69*, 1961–1973. https://doi.org/10.1016/j.gca.2004.09.003

Yu, S. Y., Colman, S. M., & Li, L. (2016). BEMMA: A hierarchical Bayesian end-member modeling analysis of sediment grain-size distributions. *Mathematical Geoscience*, *48*, 723–741. https://doi.org/10.1007/s11004-015-9611-0

Zhang, X., Wang, H., Xu, S., & Yang, Z. (2020). A basic end-member model algorithm for grain-size data of marine sediments. *Estuarine, Coastal and Shelf Science*, *236*, 106656. https://doi.org/10.1016/j.ecss.2020.106656

SUPPORTING INFORMATION

Additional supporting information can be found online in the Supporting Information section at the end of this article.

How to cite this article: Lake, N. F., Martínez-Carreras, N., Shaw, P. J., & Collins, A. L. (2022). Using particle size distributions to fingerprint suspended sediment sources—Evaluation at laboratory and catchment scales. *Hydrological Processes*, *36*(10), e14726. https://doi.org/10.1002/hyp.14726